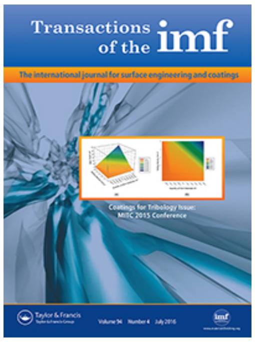

Transactions of the IMF

The International Journal of Surface Engineering and Coatings

ISSN: 0020-2967 (Print) 1745-9192 (Online) Journal homepage: http://www.tandfonline.com/loi/ytim20

White layer thickness prediction in wire-EDM using CuZn-coated wire electrode – ANFIS modelling

I. Maher, A. A. D. Sarhan, H. Marashi, M. M. Barzani & M. Hamdi

To cite this article: I. Maher, A. A. D. Sarhan, H. Marashi, M. M. Barzani & M. Hamdi (2016) White layer thickness prediction in wire-EDM using CuZn-coated wire electrode – ANFIS modelling, Transactions of the IMF, 94:4, 204-210

To link to this article: http://dx.doi.org/10.1080/00202967.2016.1180847

Published online: 13 Jul 2016.

White layer thickness prediction in wire-EDM using CuZn-coated wire electrode – ANFIS modelling

I. Maher*[1,2], A. A. D. Sarhan[1,3], H. Marashi[1], M. M. Barzani[1] and M. Hamdi[1]

Wire cutting electrical discharge machining (WEDM) is a non-traditional technique by which the required profile is acquired using spark energy. Concerning wire cutting, precision machining is necessary to achieve high product quality. White layer thickness (WLT) is one of the most important factors for evaluating surface quality. Furthermore, WLT is among the most critical constraints in cutting parameters selection in WEDM. In this research, the adaptive neuro-fuzzy inference system (ANFIS) was used to predict the WLT in WEDM using a coated wire electrode. Experimental runs were conducted to validate the ANFIS model. The predicted data were compared with measured values, and the average prediction error for WLT was 2.61%. Based on the ANFIS model, minimum WLT is achieved at the lowest levels of peak current and pulse on-time with high level of pulse off-time.

Keywords: WEDM, WLT, Neuro-fuzzy, Surface quality, Spark energy, Coated wire, HAZ

Introduction

Wire electrical discharge machining (WEDM) is among the more widely known and applied non-traditional machining processes in industry today. WEDM can machine harder, corrosion resistant, wear resistant and difficult-to-machine materials such as tool steel, titanium alloys, metal matrix composites and cemented carbides.[1] In addition, some WEDM work has also been reported on insulating ceramics and non-conductive materials.[2,3] With WEDM, it is also possible to machine complicated shapes that cannot otherwise be achieved using traditional machining processes, such as turning, milling and grinding.[4,5]

Surface quality is the most important performance parameter in WEDM which is expressed through surface roughness and WLT. In the WEDM process, WLT plays a vital role on the operational characteristics of the part (e.g. fatigue, corrosion, creep life, fracture resistance, surface friction and coating ability).

The white layer is the layer that has been heated to the melting point, but not quite hot enough to be ejected into the gap between the wire electrode and workpiece and be flushed away. The WEDM process has actually changed the metallurgical structure and characteristics in this layer as it is formed by the unejected molten metal being rapidly cooled by the dielectric fluid during the flushing process and resolidifying in the cavity. This layer does include some expelled particles that have solidified and been re-deposited on the surface before being flushed out of the gap. The white layer is densely infiltrated with carbon to the point that its structure is definitely different to that of the base material. This carbon enrichment occurs when the hydrocarbons of the electrode and dielectric fluid break down during the WEDM process and penetrate into the white layer while the material is essentially in its molten state.

Levy and Maggi[6] showed that during WEDM, a thin heat-affected zone thickness of 1 μm at 5 μJ spark energy to 25 μm at high spark energy is shaped. Moreover, the zone under the machined surface will be annealed producing the white layer. The WLT is proportionate to the discharge energy in the WEDM machining process. It is almost 50 μm for finish machining to around 200 μm for high cutting speed.[7,8]

To achieve low WLT value, the part must be machined more than once. Therefore, the desired WLT is usually specified, and proper processes are selected to reach the desired quality.[7] Actual WLT monitoring can be accomplished either by intensive post-process inspection or a prediction system. Although post-process inspection is the easiest to implement, it cannot prevent the parts from being processed before a defective batch is discovered. Moreover, WEDM is a complex machining process controlled by many process parameters. Any slight variations in one of the process parameters can affect the WLT. The most effective machining strategy is determined by identifying the different factors affecting the WEDM process, and seeking the different methods of obtaining the best machining condition and performance.[9,10]

[1]Faculty of Engineering, Department of Mechanical Engineering, Centre of Advanced Manufacturing and Material Processing (AMMP), University of Malaya, 50603 Kuala Lumpur, Malaysia
[2]Faculty of Engineering, Department of Mechanical Engineering, Kafrelsheikh University, Kafrelsheikh 33516, Egypt
[3]Faculty of Engineering, Department of Mechanical Engineering, Assiut University, Assiut 71516, Egypt

*Corresponding author, email ibrahemmaher@eng.kfs.edu.eg

Published by Taylor & Francis on behalf of the Institute
Received 24 August 2015; accepted 10 November 2015
DOI 10.1080/00202967.2016.1180847

Ultimately, the WLT prediction system can be used to obtain the best machining conditions and to determine the WLT indirectly.[11,12]

To achieve an efficient machining, prediction modelling between input WEDM parameters and output performance characteristics should be available. Soft computing techniques (fuzzy, neural network, adaptive neuro-fuzzy inference system (ANFIS), etc.) are useful when exact mathematical information is not available. In contrast to traditional computing, these techniques suffer from approximation, partial truth, met heuristics, uncertainty and inaccuracy. ANFIS is one of the soft computing techniques that play an important role in input–output parameter relationship modelling.[13,14] Maher *et al.*[15,16] used the ANFIS technique to predict the surface roughness for intelligent machining with average accuracy of 96.65 and 94%, respectively. ANFIS was also used to develop a prediction model of the WLT and the average surface roughness achieved as a function of the process parameters in WEDM.[17,18]

Hence, the aim of this work is to obtain best machining parameters (pulse on-time, pulse off-time, peak current, wire tension and wire speed) to minimise WLT of AISI 1050 carbon steel in WEDM. ANFIS prediction modelling was used to accomplish this objective.

Experimental work

Experimental design

The design of experiment (DOE) is one of the most powerful tools for experimental planning. It can be used as a great leverage to reduce experimental design changes and design cost as well as increase design process speed by using statistical methods. The Taguchi method is a most important DOE that provides a simple, systematic and efficient approach to determine the optimum process parameters. The Taguchi method applies an orthogonal array DOEs and selects a large number of control factors with a reduced number of experiments. In this array, the control factor matrix ensures a balanced contrast between the level and independent distribution among parameters.[19] The Taguchi L18 orthogonal array was selected because of the four machining variables with three levels and one machining variable with two levels, as shown in Table 1.

The machining parameters including peak current (I_P), pulse on-time (T_{on}), pulse off-time (T_{off}), wire speed (W_S) and wire tension (W_T) were chosen in this study to investigate the effect on machining performance including WLT. The machining parameters' levels were chosen according to previous experiments with the working range and levels of the WEDM process parameters by using the one-factor-at-a-time approach. The 18 experiments were arranged with combinations of each level and control factor in an orthogonal array matrix assigned using MINITAB 15 software, as shown in Table 2. The other machining parameters were kept constant as a fixed value during experiments as recommended by the machine maker to optimise the process such as gap voltage = 20 V; flush pressure = 14 kgf cm^{-2}; and water resistivity = 6×10^4 Ω cm.

Table 1 Levels of machining parameters

Machining parameter	Symbol	Units	Levels		
			1	2	3
Peak current	IP	A	16	17	–
Pulse on time	T_{on}	μs	0.2	0.3	0.4
Pulse off time	T_{off}	μs	0.5	0.9	1.3
Wire tension	WT	G	350	600	1050
Wire speed	WS	m min^{-1}	3	7	11

Table 2 Combination of parameters of the mixed orthogonal array L18 experimental plan

Exp. no.	Parameters' combination				
	IP	T_{on}	T_{off}	WT	WS
1	1	1	1	1	1
2	1	1	2	2	2
3	1	1	3	3	3
4	1	2	1	1	2
5	1	2	2	2	3
6	1	2	3	3	1
7	1	3	1	2	1
8	1	3	2	3	2
9	1	3	3	1	3
10	2	1	1	3	3
11	2	1	2	1	1
12	2	1	3	2	2
13	2	2	1	2	3
14	2	2	2	3	1
15	2	2	3	1	2
16	2	3	1	3	2
17	2	3	2	1	3
18	2	3	3	2	1

Experimental set-up

The experiments were performed using a computer numerical control Sodick A500W WEDM machine tool. Coated wire electrode (Brass wire core (60/40) coated with 5 μm of CuZn alloy (30/70)) with tensile strength of 875 N mm^{-2}, diameter of 0.2 mm, elongation of 0.2 and electrical conductivity of 20% ICAS (delivered by Sunrox EDM supplier) was used for machining blocks of AISI 1050 carbon steel under specific machining conditions (Table 1).

Sample preparation

The workpiece material (AISI 1050 carbon steel with $100 \times 100 \times 20$ mm dimensions) was machined into $5 \times 5 \times 20$ mm for each specimen. The chemical composition was achieved by EDX analysis and is given in Table 3. The electrical resistivity and thermal conductivity of AISI 1050 carbon steel were taken as 1.63×10^{-5} Ω cm and 49.8 W (m K)$^{-1}$, respectively.

The samples were ground using 120 SiC abrasives for stock removal requirements. Once planarity and the area of interest were obtained, a standard grit silicon carbide paper P220 (30 s), P360 (30 s), P800 (30 s), P1200 (60 s), P2400 (90 s), P4000 (120 s), with pressure of around 10 N, counter rotation of 400 rev min^{-1} and

Table 3 Elemental analysis of AISI 1050 carbon steel by EDX

Element	*C*	Mn	*P*	*S*	Fe
%	0.54	0.69	0.03	0.04	98.7

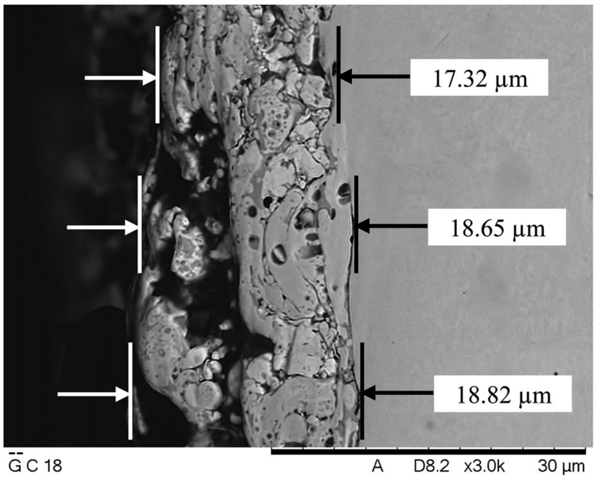

1 Measurement of WLT (SEM micrograph of sample No. 18)

plenty of coolant water were applied. The samples were cleaned in ethanol using an ultrasonic agitator between the steps at 30°C for 15 min. Then the samples were roughly polished using 6 and 3 μm diamond suspension liquid with pressure of 6 N and 5 min counter rotation of 400 rev min^{-1}. The process was repeated until the surface was smooth (checked with optical microscope (OM), interference contrast mode). Finally, 0.05 μm alumina suspension liquid, with pressure 5 N, was used for final polishing with 400 rev min^{-1} counter rotation for 5 min. The final polishing process was repeated until the microstructure was clearly visible (checked with OM). Then the sample surfaces were washed with distilled water, flushed with ethanol and dried with a hair dryer. The samples were then cleaned in an ultrasonic agitator in acetone at 30°C for 15 min, carefully rinsed and cleaned in ethanol, and dried to remove contamination so as to acquire a uniform surface.[20] All materials and reagents used in sample preparation were provided by the surface laboratory, Faculty of Engineering, University of Malaya.

Surface characterisation

Microscopic surface examinations after each grinding and finishing step were carried out using Olympus BX 61 light OM. A scanning electron microscope (SEM) equipped with energy-dispersive X-ray spectroscopy (Hitachi tabletop microscope TM3030) was used to examine the surface microstructural and topographical characteristics and WLT of the machined part.

Experimental results and ANFIS modelling

Experimental results

The average WLT was calculated for three different measurements at three different places using an image processing programme (ImageJ) as shown in Fig. 1. Eighteen sets of data were used based on DOEs for building and training the ANFIS model, as shown in Table 4. As shown in Table 4, the standard deviations (S) for all samples are small, meaning the measured values tend to be close to their mean. The other four sets were used for testing, once training was completed, to verify the accuracy of the predicted WLT values.

ANFIS model construction

The neuro-fuzzy system combines the advantage of fuzzy systems which deal with explicit knowledge that can be explained and understood, with neural networks which deal with implicit knowledge that can be acquired only through learning.[21] To enable a system to deal with cognitive uncertainties in a manner more like humans, one may incorporate the concept of fuzzy logic into the neural networks.

ANFIS was constructed through MATLAB, and 18 readings comprised the training data set as listed in Table 4. Two membership functions of peak current and three membership functions of the other parameters (pulse on-time, pulse off-time, wire speed and wire tension) were chosen for creating the ANFIS model. The

Table 4 Measured WLT/μm at different machining conditions

Machining parameters					Performance characteristics				
					WLT/μm				
IP/A	T_{on}/μs	T_{off}/μs	WT/g	WS/m min^{-1}	1	2	3	S	Avg.
16	0.2	0.5	350	3	7.93	8.39	9.01	0.542	8.44
		0.9	600	7	7.34	6.95	6.47	0.436	6.92
		1.3	1050	11	5.72	5.1	5.67	0.344	5.50
	0.3	0.5	350	7	15.79	15.88	14.84	0.576	15.50
		0.9	600	11	13.67	13.91	12.93	0.511	13.50
		1.3	1050	3	10.72	11.58	10.79	0.478	11.03
	0.4	0.5	600	3	21.5	19.79	21.18	0.909	20.82
		0.9	1050	7	19.47	18.53	17.53	0.970	18.51
		1.3	350	11	16.32	15.91	16.18	0.208	16.14
17	0.2	0.5	1050	11	11.74	12.53	11.03	0.750	11.77
		0.9	350	3	10.88	11	10.27	0.391	10.72
		1.3	600	7	8.68	9.88	9.97	0.720	9.51
	0.3	0.5	600	11	17.82	17.38	16.79	0.517	17.33
		0.9	1050	3	15.13	14.26	15.79	0.767	15.06
		1.3	350	7	13.62	12.53	13.24	0.553	13.13
	0.4	0.5	1050	7	23.24	22.68	23.82	0.570	23.25
		0.9	350	11	20.24	19.15	20.59	0.751	19.99
		1.3	600	3	17.32	18.65	18.82	0.821	18.26

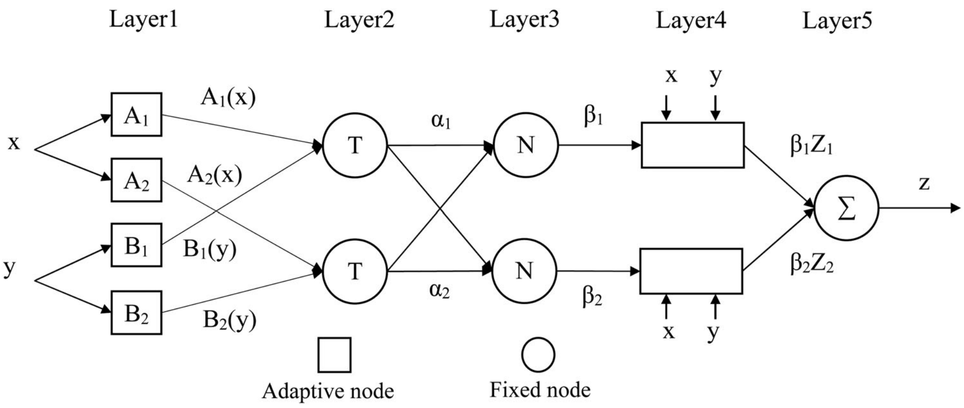

2 ANFIS architecture for the two-input Sugeno fuzzy model

generalised bell membership function (gbellmf) was adopted for the ANFIS training process in this study. The fuzzy rule architecture of ANFIS when gbellmf is adopted consists of 18 fuzzy rules generated from the input–output data set based on the Sugeno fuzzy model. During training, the 18 performance measure values were used to conduct 50 cycles of learning with an average error of 1.44×10^{-5}.

ANFIS uses five network layers to build the model. To explain this model simply, we have assumed only two rules, and two linguistic values for each input variable as shown in Fig. 2.

Layer 1: The output of this layer is the degree to which the given input satisfies the linguistic label associated with this node. Generalised bell-shaped membership functions (gbellmf) are normally used to denote the linguistic terms because the relationship between the cutting parameters and WLT in WEDM is not linear, as shown in Fig. 3*a*. A generalised bell membership function is specified by three parameters (a, b, c) as shown in equations (1) and (2). The parameter *b* is usually positive and used to control the slope of the crossover point. Moreover, parameters *a* and *c* control the centre and width of the membership function.

$$A_i(x) = \frac{1}{1 + \left|\frac{x - c_{i1}}{{}_{i1}}\right|^{2b_{i1}}} \tag{1}$$

$$B_i(y) = \frac{1}{1 + \left|\frac{y - c_{i2}}{a_{i2}}\right|^{2b_{i2}}} \tag{2}$$

where (a_{i1}, a_{i2}, b_{i1}, b_{i2}, $c_{i1,}$ c_{i2}) is the parameter set.

When the values of the parameter set change, the bell-shaped functions differ consequently (Fig. 3*b*), thus displaying several forms of membership functions on linguistic labels A_i, and B_i.

Layer 2: Each neuron in this layer computes the firing strength of the associated rule. The outputs of the top and bottom nodes are as follows:

$$\alpha_1 = A_1(x) \times B_1(y) = A_1(x) \wedge B_1(y) \tag{3}$$

$$\alpha_2 = A_2(x) \times B_2(y) = A_2(x) \wedge B_2(y) \tag{4}$$

Both nodes in this layer are labelled by *T*, because we can choose other *t*-norms for modelling the logical and operator. The nodes of this layer are called rule nodes.

Layer 3: Each neuron in this layer computes the normalisation of the firing levels. The outputs of the top and bottom neurons are the normalised firing level of the first and second rules, respectively.

$$\beta_1 = \frac{\alpha_1}{\alpha_1 + \alpha_2} \tag{5}$$

$$\beta_2 = \frac{\alpha_2}{\alpha_1 + \alpha_2} \tag{6}$$

Layer 4: Each neuron in this layer computes the product of the normalised firing levels with the outputs of an individual associated rule.

$$\beta_1 Z_1 = \beta_1(a_1 x + b_1 y) \tag{7}$$

$$\beta_2 Z_2 = \beta_2(a_2 x + b_2 y) \tag{8}$$

Layer 5: The neuron in this layer computes the sum of all incoming values.

$$Z = \beta_1 Z_1 + \beta_2 Z_2 \tag{9}$$

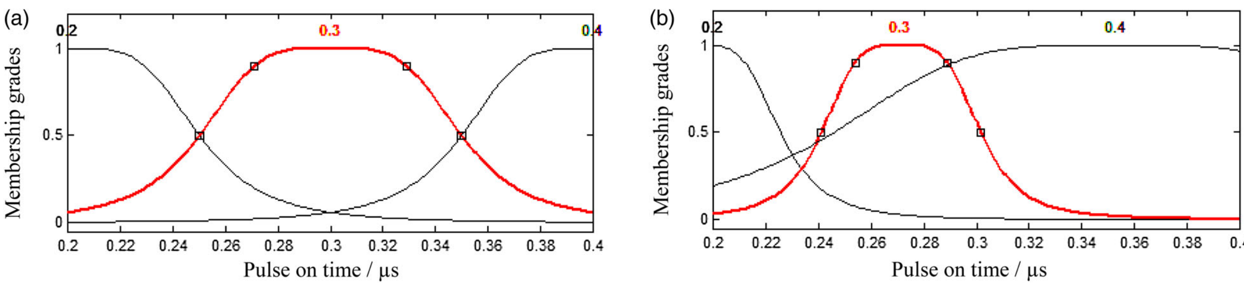

3 Initial and final membership functions of pulse on-time, *a* initial membership function, *b* final membership function after training

Table 5 The measured vs. predicted WLT of the testing data set

Machining parameters					WLT		
IP/A	T_{on}/μs	T_{off}/μs	WT/g	WS/m min^{-1}	Measured	Predicted (ANFIS)	Error/%
16	0.25	0.7	475	5	13.63	13.4	1.69
	0.35	1.1	825	9	16.8	16.4	2.38
17	0.25	0.7	475	5	12.72	11.8	7.23
	0.35	1.1	825	9	17.86	17.8	0.34
Average percentage error/%							2.91

If a crisp training set $((x^k, y^k), k = 1, \ldots, K)$ is given, then the parameters of the hybrid neural net can be learned by descent-type methods. The error function for pattern k is given by

$$E_k = (O^k - Z^k)^2 \quad (10)$$

where O^k is the desired output and Z^k is the calculated output by the neural network.

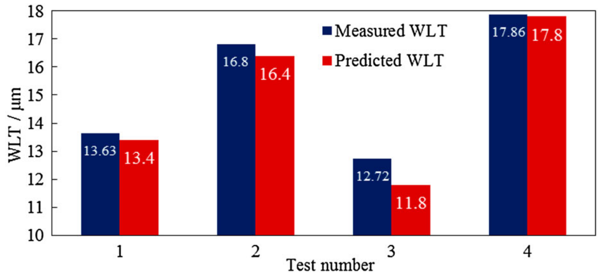

4 Comparison of measured and predicted WLT of the testing data set

ANFIS model verification

Four random readings were used as the testing data set. The measured WLT values *vs.* predicted values using the ANFIS model are given in Table 5. The plot of four measured WLT values *vs.* predicted values using the ANFIS model is shown in Fig. 4. This figure presents a comparison of the measured and predicted WLT of AISI 1050 carbon steel using the coated wire electrode. Appropriate assent is evident between the measured and predicted values. This close assent obviously displays that the ANFIS models can be used to predict and optimise the WLT under consideration.

To evaluate the fuzzy model, the percentage error E_i and average percentage error E_{av} defined in equations

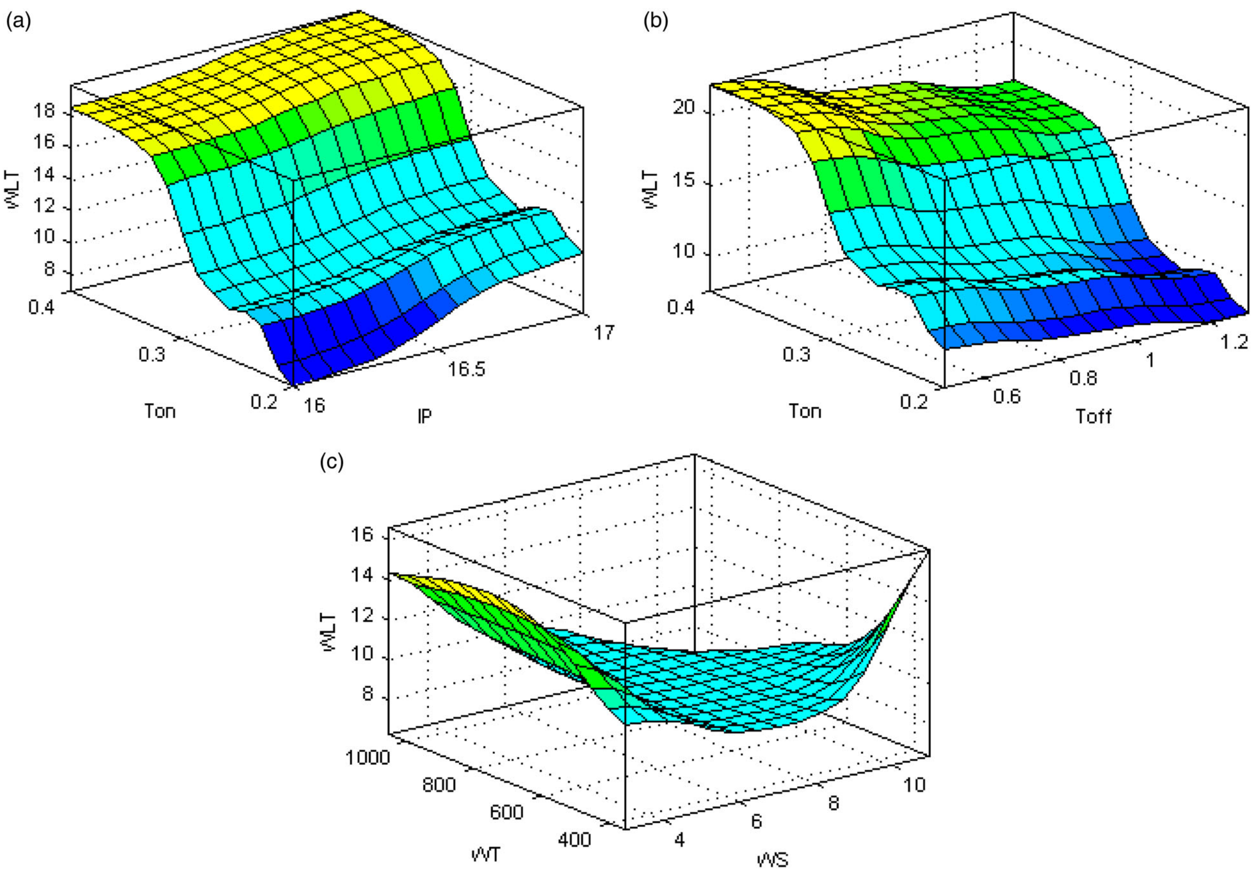

5 The modelled WLT by ANFIS in relation to cutting parameters change, *a* WLT in relation to change of pulse on-time and peak current, *b* WLT in relation to change of pulse on-time and pulse off-time and *c* WLT in relation to change of wire tension and wire speed.

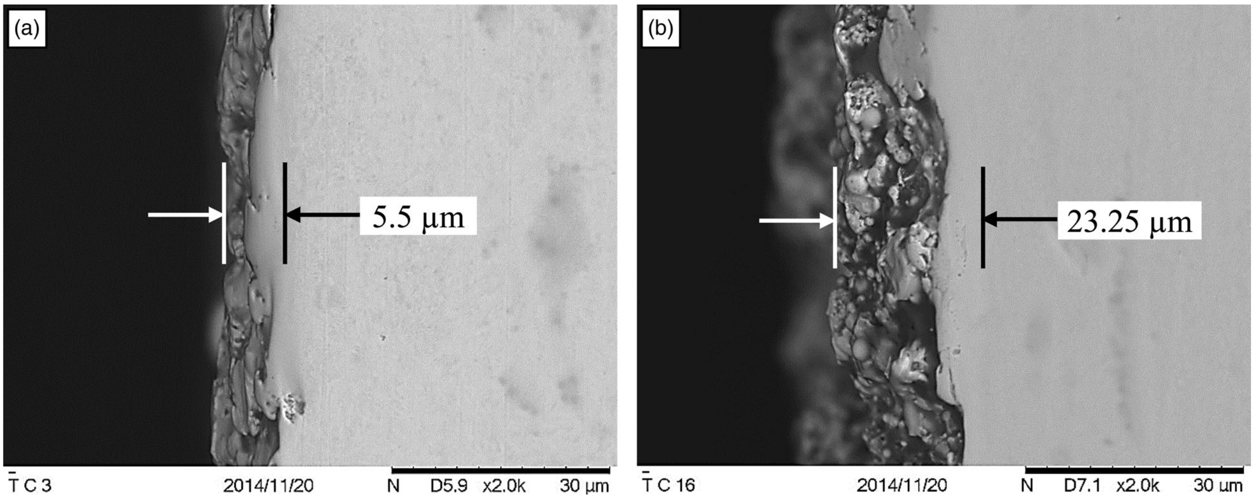

6 SEM micrographs of the workpiece edge at the extreme levels of spark energy, *a* at peak current 16 A, pulse on-time of 0.2 µs and pulse off-time of 1.3 µs, *b* at peak current of 17 A, pulse on-time of 0.4 µs and pulse off-time of 0.5 µs

(11) and (12), respectively, were used.

$$E_i = \frac{|T_m - T_p|}{T_m} \times 100 \qquad (11)$$

$$E_{av} = \frac{1}{m}\sum_{i=1}^{m} E_i \qquad (12)$$

where T_m is the measured WLT; T_p is the predicted value; and $i = 1,2,3,4$ is the sample number.

The obtained average percentage error is 2.91% (Table 5). The low error level signifies that the WLT results predicted by ANFIS are very close to the actual experimental results. The error values mean that the proposed model can predict and optimise the WLT satisfactorily.

ANFIS model results and discussion

Figure 5 introduces the modelled WLT by ANFIS in relation to change in cutting parameters. It is clear from the figure that the peak current, pulse on-time and pulse off-time have a great effect on WLT but the wire tension and speed have a minor effect on the WLT. Figure 5*a* and *b* shows that the WLT increases with increasing peak current and pulse on-time but decreases with increasing pulse off-time. Moreover, WLT slightly decreases with increasing wire tension and speed as shown in Fig. 5*c*. This is because the combination of pulse on-time and peak current determine the spark energy (equation (13))[7] and hence the amount of heat required to melt or evaporate the workpiece surface.

$$E_s = \mathrm{IP} \times V \times T_{on} \qquad (13)$$

where E_s is the spark energy and V is the spark gap set voltage.

Figure 6*a* and *b* introduces SEM micrographs at 2000× magnification of the white layer for sample numbers 3 and 16, respectively. These micrographs verify that the maximum width of the white layer is at the highest levels of peak current, pulse on-time and the lowest level of pulse off-time. This is because the heat energy increases with peak current and pulse on-time. In addition, the number of pulses increases with decreasing pulse off-time. Hence, greater heat is produced on the machined surface and leads to greater WLT on the workpiece. Based on ANFIS modelling, using low peak current and pulse on-time with high pulse off-time yields the best conditions for better cutting and low WLT.

Conclusion

ANFIS were used to develop an empirical model for predicting the WLT in WEDM. Pulse on-time, pulse off-time, peak current, wire speed and wire tension were used as predictor variables. Eighteen measured WLT values, under different cutting conditions, were used as a training data set to build the ANFIS model and four values were used as a testing data set. The model was verified with test data where the average errors were 2.61%. These results indicate that the ANFIS model with gbellmf is accurate and can be used to predict WLT in WEDM. The ANFIS model shows the peak current, pulse on-time and pulse off-time are the most significant parameters affecting the WLT. The wire tension and wire speed have a minor effect on the WLT. The ANFIS model shows that minimum WLT is achieved at the lowest levels of peak current and pulse width with the highest level of pulse off-time.

Acknowledgement

The authors would like to acknowledge the University of Malaya for providing the necessary facilities and resources for this research. This research was funded by the University of Malaya Research Grant (UMRG) Program No. RP039B-15AET and Postgraduate Research Grant (PPP) Program No. PG020-2013B. The extended abstract of this research work was originally accepted for and presented at the Malaysian International Tribology Conference (MITC2015), Penang, Malaysia, 16–17 November 2015.

ORCiD

I. Maher http://orcid.org/0000-0003-3947-9971

References

1. N. Patil and P. K. Brahmankar: 'Determination of material removal rate in wire electro-discharge machining of metal matrix composites using dimensional analysis', *Int. J. Adv. Manuf. Technol.*, 2010, **51**, (5–8), 599–610.
2. A. Sabur, M. Y. Ali, M. A. Maleque and A. A. Khan: 'Investigation of material removal characteristics in EDM of nonconductive ZrO_2 ceramic', *Procedia Eng.*, 2013, **56**, 696–701.
3. R. Wüthrich and V. Fascio: 'Machining of non-conducting materials using electrochemical discharge phenomenon–an overview', *Internat. J. Machine Tools Manuf.*, 2005, **45**, (9), 1095–1108.
4. C. Sommer and S. Sommer: 'Complete EDM handbook', 2013, Houston, TX, Reliable EDM.
5. X. Cheng, X. H. Yang, Y. M. Huang, G. M. Zheng and L. Li: 'Helical surface creation by wire electrical discharge machining for micro tools', *Robot Comput.-Int. Manuf.*, 2014, **30**, (3), 287–294.
6. G. N. Levy and F. Maggi: 'WED machinability comparison of different steel grades', *CIRP Ann. – Manuf. Technol.*, 1990, **39**, (1), 183–185.
7. H. El-Hofy: 'Advanced machining processes', 2005, New York, McGraw-Hill.
8. J. A. McGeough: 'Electrodischarge machining' in 'Advanced methods of machining', 1988, New York, Springer.
9. R. Garg: 'Effect of process parameters on performance measures of wire electrical discharge machining', Ph.D. thesis, National Institute of Technology, Kurukshetra, 2010.
10. J. T. Huang, Y. S. Liao and W. J. Hsue: 'Determination of finish-cutting operation number and machining-parameters setting in wire electrical discharge machining', *J. Mater. Proc. Technol.*, 1999, **87**, (1–3), 69–81.
11. I. Maher, L. H. Ling, A. A. D. Sarhan and M. Hamdi: 'Improve wire EDM performance at different machining parameters – ANFIS modeling', *IFAC-PapersOnLine*, 2015, **48**, (1), 105–110.
12. M. Shabgard, S. Oliaei, M. Seyedzavvar and A. Najadebrahimi: 'Experimental investigation and 3D finite element prediction of the white layer thickness, heat affected zone, and surface roughness in EDM process', *J. Mech. Sci. Technol.*, 2011, **25**, (12), 3173–3183.
13. A. Sarkheyli, A. Zain and S. Sharif: 'A multi-performance prediction model based on ANFIS and new modified-GA for machining processes', *J. Intell. Manuf.*, 2015, **26**, (4), 703–716.
14. I. Maher, M. E. H. Eltaib, A. D. Sarhan and R. M. El-Zahry: 'Cutting force-based adaptive neuro-fuzzy approach for accurate surface roughness prediction in end milling operation for intelligent machining', *Int. J. Adv. Manuf. Technol.*, 2015, **76**, 1459–1467.
15. I. Maher: 'Surface Roughness Prediction in End-Milling Process', M. Sc. thesis, Assiut University, Assiut, Egypt, 2008.
16. I. Maher, M. E. H. Eltaib and R. M. El-Zahry: 'Surface roughness prediction in end milling using multiple regression and adaptive neuro-fuzzy inference system', Int Conf. on Mechanical Engineering Advanced Technology for Industrial Production (MEATIP4), Assiut University, Egypt, 12–14 December 2006, 614–620.
17. U. Çaydaş, A. Hasçalık and S. Ekici: 'An adaptive neuro-fuzzy inference system (ANFIS) model for wire-EDM', *Expert Syst. Appl.*, 2009, **36**, (3, Part 2), 6135–6139.
18. I. Maher, A. A. D. Sarhan, M. M. Barzani and M. Hamdi: 'Increasing the productivity of the wire-cut electrical discharge machine associated with sustainable production', *J. Clean Prod.*, 2015, **108**, Part A, 1 December, 247–255.
19. R. K. Roy: 'Design of experiments using Taguchi approach: 16 steps to product and process improvement', 2001, New York, John Wiley & Sons, Inc.
20. D. C. Zipperian: 'Metallographic handbook', 2011, Tuscon, AZ, PACE Technologies.
21. H. Li, C. L. P. Chen and H. P. Huang: 'Fuzzy neural intelligent systems: Mathematical foundation and the applications in engineering', 2001, London, CRC Press LLC.